Gold Nanoparticles and Microwave Irradiation Inhibit Beta-Amyloid Amyloidogenesis

Eyleen Araya · Ivonne Olmedo · Neus G. Bastus · Simón Guerrero · Víctor F. Puntes · Ernest Giralt · Marcelo J. Kogan

Abstract Peptide-Gold nanoparticles selectively attached to β-amyloid protein (Aβ) amyloidogenic aggregates were irradiated with microwave. This treatment produces dramatic effects on the Aβ aggregates, inhibiting both the amyloidogenesis and the restoration of the amyloidogenic potential. This novel approach offers a new strategy to inhibit, locally and remotely, the amyloidogenic process, which could have application in Alzheimer's disease therapy. We have studied the irradiation effect on the amyloidogenic process in the presence of conjugates peptide-nanoparticle by transmission electronic microscopy observations and by Thioflavine T assays to quantify the amount of fibrils in suspension. The amyloidogenic aggregates rather than the amyloid fibrils seem to be better targets for the treatment of the disease. Our results could contribute to the development of a new therapeutic strategy to inhibit the amyloidogenic process in Alzheimer's disease.

Keywords Alzheimer's disease · Therapy · Aggregation · Toxicity · Nanobiotechnology

Introduction

Protein misfolding and aggregation in general and amyloidogenesis in particular are of growing interest as scientists recognize their role in devastating degenerative diseases

E. Araya
Instituto de Medicina Molecular Aplicada, Sinclair 3106, Ciudad Autónoma de Buenos Aires, CP 1425FRF, Argentina

E. Araya
University of Barcelona, Barcelona, Spain

I. Olmedo · S. Guerrero · M. J. Kogan
Facultad de Ciencias Químicas y Farmacéuticas, Universidad de Chile, Olivos 1007, Independencia, Santiago, Chile

N. G. Bastus · V. F. Puntes
Institut Català de Nanotecnologia, Campus UAB, 08193 Barcelona, Spain

N. G. Bastus
Departament de Física Fonamental, Universitat de Barcelona, 08028 Barcelona, Spain

S. Guerrero
Universidad de Santiago de Chile, Santiago, Chile

V. F. Puntes
Institut Català de Recerca i Estudis Avançats (ICREA), 08093 Barcelona, Spain

E. Giralt
Design Synthesis and Structure of Peptides and Proteins, Institute for Research in Biomedicine (IRB Barcelona), 08028 Barcelona, Spain

E. Giralt
Department of Organic Chemistry, University of Barcelona, 08028 Barcelona, Spain

M. J. Kogan (✉)
Centro para la Investigación Interdisciplinaria Avanzada en Ciencias de Materiales, Santiago, Chile
e-mail: mkogan@ciq.uchile.cl

such as Alzheimer's and Parkinson's disease. Protein and peptide aggregation into mature amyloid fibrils is a multistep process initiated by conformational changes with samplings of prefibrillar intermediate amyloidogenic aggregates (PIAA), such as oligomers, protofibrils, pores, amylospheroids, and short fibrils [1]. Alzheimer′s disease is a neurodegenerative disorder characterized by the presence of extracellular deposits of amyloid protein and plaques in the brain, composed primarily of toxic aggregates (PIAA and amyloid fibrils) of β-amyloid protein (Aβ) [2]. In a recent report, we demonstrated the feasibility of remote deposit redissolving by using the local heat dissipated by gold nanoparticles (AuNP) selectively attached to the Aβ fibrils when irradiated with microwaves (MW) [3–5]. Although the mature fibril was once assumed to be the biologically toxic species, it has recently been hypothesized that soluble intermediates such as PIAA are most damaging [6–8]. Recently, several authors have hypothesized that the key to an early pathogenic event in the onset of Alzheimer's disease is likely the formation of amyloidogenic species rather than the amyloid fibrils. A strategy for the treatment of the disease could be reducing the amyloidogenicity of this species [9, 10]. In an early stage, this inhibition is of major importance to develop a potential strategy for treating the Alzheimer's disease. Thus, the current study intends to demonstrate that the inhibition of the aggregation process of β-amyloid in vitro by applying weak microwave fields (0.1 W) is possible in the presence of AuNP.

Could MW and AuNP Treatment Halt the Amyloidogenic Process of PIAA?

Medical application of MW began in the 1970s [11]. In animals and humans, local MW exposure stimulates tissue repair and regeneration, alleviates stress reactions, and facilitates recovery in a wide range of diseases [12]. MW also modulates the effect of X-rays at both cellular and organism levels. Diseases reported to be successfully treated with MW are gastric, duodenal ulcers, cardiovascular diseases, respiratory sickness, tuberculosis, skin diseases, etc. [13]. MW irradiation with low-power density also stimulates the immune potential of macrophages and T cells [14]. On the other side, more intense MW fields produce effects such as conformational changes and denaturation processes on proteins [15]. The use of MW and AuNP to produce local and remote heating is a powerful tool for the development of new strategies to manipulate the aggregation state of toxic proteins [3, 4]. Irradiation has been extensively explored as a means of remote heating of biological tissues mediated by inorganic nanoparticles [16]. In this study, we selectively bound AuNP to Aβ_{1-42} PIAA (Aβ PIAA) and investigated the effect of MW irradiation on the amyloidogenic process. To allow selective attachment to PIAA, AuNPs were linked to peptide CLPFFD, which contains the LPFFD sequence that attaches selectively to the amyloidogenic Aβ_{1-42} structures, forming the conjugate AuNP-CLPFFD. LPFFD recognizes a particular (hydrophobic) domain of the β-sheet structure [17].

Methods

CLPFFD Synthesis

CLPFFD was synthesized following fluorenylmethyloxycarbonyl (Fmoc) strategy and solid phase synthesis where the peptide is C-termed with an amide (CLPFFD-NH_2). Fmoc-protected amino acids were purchased from Novabiochem (Laufelfingen, Switzerland) and Perseptive Biosystems (Framingham, Massachusetts). O-(Benzotriazol-1-yl)-*N*,*N*,*N*′,*N*′-tetramethyluronium tetrafluoroborate (TBTU), Fmoc-AM handle, and resin MBHA were also obtained from Novabiochem. Chemical reagents *N*,*N*′-diisopropylcarbodiimide (DIPCI), 1-Hydroxy-1H-Benzotriazole (HOBt), triethylsilane, and dimethylaminopyridine (DMAP) were from Fluka (Buchs, Switzerland). Manual synthesis included the following steps: (i) resin washing with DMF (5 × 30 s); (ii) Fmoc removal with 20% piperidine/DMF (1 × 1 min + 2 × 7 min); (iii) washing with DMF (5 × 30 s); (iv) washing with DMF (5 × 30 s) and CH_2Cl_2 (5 × 30 s); (v) Kaiser's test (with a peptide-resin sample); (vi) DMF washing (5 × 30 s). Cleavage of the peptide was carried out by acidolysis with trifluoroacetic acid (TFA) using triethylsilane and water as scavengers (94:3:3, v/v/v) for 60–90 min. TFA was removed with N_2 stream and the oily residue precipitated with dry tert-butyl ether. Peptide crude was recovered by centrifugation and decantation of the tert-butyl ether phase. The solid was redissolved in (water:acetonitrile 1:1) and lyophilized. The peptide was analyzed by RP-HPLC [Waters 996 photodiode array detector (λ = 443 nm) equipped with a Waters 2695 separation module (Milford, MA), a Symmetry column (C18, 5 µm, 4.6 × 150 mm), and Millennium software; flow rate = 1 mL/min, gradient = 5–100% B over 15 min (A = 0.045% TFA in H_2O, and B = 0.036% TFA in acetonitrile)]. The peptide was purified by semipreparative RP-HPLC [Waters 2487 Dual Absorbance Detector equipped with a Waters 2700 Sample Manager, a Waters 600 Controller, a Waters Fraction Collector, a Symmetry column (C18, 5 µm, 30 × 100 mm^2), and Millennium software]. The peptide was finally characterized by amino acid analysis with a Beckman 6300 analyzer and by MALDI-TOF with a Bruker model Biflex III. The result

of the amino acid analysis of CLPFFD-NH_2 was Asp 1.0 (1), Pro 0.97 (1), Leu 1.0 (1), Phe 2.03 (2), and in the mass spectrum MALDI-TOF of CLPFFD-NH_2, the peaks $[M^+H^+] = 740$ and $[M^+Na^+] = 762$ were found.

AuNP Synthesis

Citrate-coated AuNP (12.5 ± 1.7 nm) were prepared by citrate reduction of $HAuCl_4$ in accordance with Ref. [4]. An aqueous solution of $HAuCl_4$ (100 mL, 1 mM) was refluxed for 5–10 min, and a warm (50–60 °C) aqueous solution of sodium citrate (10 mL, 38.8 mM) was added quickly [3]. Reflux was continued for another 30 min until a deep red solution appeared. The solution was filtered through 0.45 μm Millipore syringe filters to remove any precipitate, the pH was adjusted to 7.4 using dilute NaOH solution, and the filtrate was stored at 4 °C. AuNPs were observed by Transmission Electronic Microscopy (TEM) using a JEOL JEM-1010 microscope. The specimen was prepared by dropping AuNP on formvar carbon-coated copper microgrids and letting them dry.

Conjugation of CLPFFD with AuNP

AuNP-CLPFFD was prepared by mixing 5 nM AuNP and peptide CLPFFD solution (1 mg/ml) in a volume ratio 10 to 1. The conjugation was made in the presence of excess peptide to ensure full conversion of the AuNP and, consequently, homogeneous conjugation. The conjugate AuNP-CLPFFD was afterwards purified first in a 450 nm filter and then by dialysis (for 3 days in a membrane Spectra/Por MWCO: 6–8000 against 1.2 mM sodium citrate and the solution was changed 6 times) to eliminate the excess of peptide. UV–vis absorption spectra were recorded at room temperature with a Unicam UV/Vis spectrophotometer (UV3). To verify that after dialysis the non-conjugated peptide was completely eliminated, two experiments were performed:

(a) After dialysis, 3 mL of AuNP-CLPFFD was centrifuged at 16,000*g* for 30 min (AuNP-CLPFFD sediments) and the supernatant was evaporated to dryness, and an analysis of amino acids and HPLC ES-MS were carried out. In both cases, the presence of the peptide was not detected.
(b) The AuNP-CLPFFD pellet obtained after dialysis and centrifugation was washed twice with 300 μL of 1% TFA. For washing, the pellet was redissolved and centrifuged at 16,000*g* for 30 min (this treatment allows the detachment of non-covalent molecules that could be retained and non-covalently attached to AuNP-CLPFFD pellet). In the supernatant, free peptide was not detected by HPLC ES-MS, which indicates that after dialysis the free peptide was completely eliminated. It is important to mention that washing with a dilute solution of trifluoroacetic acid, 1% TFA, does not provoke the cleavage of CLPFFD from the AuNP-CLPFFD conjugate.

Characterization of Conjugates AuNP-CLPFFD

X-ray photoelectron spectroscopy (XPS) experiments were performed in a PHI 5500 multitechnique System (from Physical Electronics) with a monochromatic X-ray source (Aluminum Kalfa line of 1486.6 eV energy and 350 W), placed perpendicular to the analyzer axis and calibrated using the 3d5/2 line of Ag with a full width at half maximum (FWHM) of 0.8 eV. The analyzed area was a circle of 0.8 mm diameter, and the selected resolution for the spectra was 187.5 eV of Pass Energy and 0.8 eV/step for the general spectra and 23.5 eV of Pass Energy and 0.1 eV/step for the spectra of the different elements. Some measurements were done after some cleaning by sputtering the surface with an Ar^+ ion source (4 keV energy). All measurements were made in an ultra high vacuum chamber pressure between 5×10^{-9} and 2×10^{-8} Torr. In AuNP-CLPFFD, the expected peaks from S 2p, S 2s, and Au 4f core levels were detected. High-resolution data have also been recorded in the S 2p, S 2s, and Au 4f, spectral regions. The S 2p signal consists of a broad band with a maximum at 162.2 eV that corresponds to the chemisorptions of sulfur grafted onto gold. The experimental curve fitted with the signals S 2p3/2 and S 2p1/2 (162.1 and 163.3 eV signals, respectively) that correspond to a doublet for sulfur atoms bound to gold (supplementary data). According to our calculations, the signal of 164 eV was not found in this peak, which led us to conclude that unbound S species are not present in the samples. In addition, the S 2s photoelectron peak was observed. This peak is a particularly good parameter since it is a singlet, thus making the interpretation straightforward. The S 2s photoelectron binding energy (BE) from bulk peptide with the free thiol and AuNP peptide thiolate are found at 228.2 and 227.3, respectively. The accuracy of these BE values is estimated to be ±0.2 eV at the worst. In the case of bare AuNP and capped AuNP, the signal corresponding to Au 4f7/2 is positioned at 84.2 eV. The fact that the measured Au 4f7/2 photoelectron BE is not detected by the sulfur chemisorption is probably because the peak separation is too small.

Estimation of the Number of Peptide Attached Molecules per AuNP

The amount of peptide molecule per NP was estimated by analysis of amino acids and absorption spectrophotometry.

The concentration of AuNP in the solutions was obtained taking into account the molar coefficient of extinction of the 12 nm diameter ($5.7 \times 107\ M^{-1}\ cm^{-1}$) AuNP and an analysis of amino acids of the pellet obtained after centrifugation of the conjugates at 13,500 rpm for 30 min (in such conditions, the NP sediment). In the amino acid analysis, a hydrolysis of the peptide conjugated to the AuNP (the non-conjugated peptide was eliminated in Section "Conjugation of CLPFFD with AuNP") was performed; thus it was possible to determine the concentration of attached peptide molecules. The number of peptide molecules per AuNP was obtained by dividing the number of peptide molecules per mL of solution by the number of particles per mL of solution. This ratio was obtained in triplicate in three independent syntheses and conjugations. The degree of conjugation of AuNP-CLPFFD is 460 ± 30 peptide molecules per AuNP.

Preparation of Aβ PIAA Solutions

$A\beta_{1-42}$ was purchased from r-Peptide (USA). About 1 mg peptide was suspended in water (1 mL) and this suspension was divided in 10 aliquots. Peptide aliquots were lyophilized in glass vials and stored at −20 °C. To obtain a homogeneous $A\beta_{1-42}$ solution free from aggregates, the peptide was treated with 200 µL of 1,1,1,3,3,3-hexafluoro-2-propanol (HFIP) for 30 min at room temperature. The HFIP was then lyophilized and the peptide was dissolved in water to obtain a 400 μM solution of Aβ PIAA [18].

Aβ PIAA/AuNP-CLPFFD and Controls for Irradiation

Sodium citrate, AuNP, AuNP-CLPFFD, or CLPFFD were added to the Aβ PIAA and the samples were incubated for 25 min at room temperature. We irradiated two samples with different ratio of Aβ/AuNP-CLPFFD (10 µM:1 nM and 10 µM:0.2 nM) and the controls.

Samples

Aβ PIAA/1 nM AuNP-CLPFFD Samples were prepared by mixing 12.5 µL of 400 µM Aβ, 100 µL of 5 nM AuNP-CLPFFD, and 388 µL of sodium citrate 1.2 mM.

Aβ PIAA/0.2 nM AuNP-CLPFFD Samples were prepared by mixing 12.5 µL of 400 µM Aβ PIAA, 20 µL of 5 nM AuNP-CLPFFD, and 468 µL of sodium citrate 1.2 mM.

Controls

For the irradiation process we used three controls: (1) Aβ PIAA, a solution of PIAA (12.5 µL of 400 µM Aβ) was mixed with 487.5 µL of sodium citrate 1.2 mM; (2) Aβ PIAA + AuNP, a solution of PIAA (12.5 µL of 400 µM Aβ) was mixed with 100 µL of 5 nM AuNP and 388 µL of sodium citrate 1.2 mM; (3) Aβ PIAA + CLPFFD, a solution of Aβ PIAA (12.5 µL of 400 µM Aβ) was mixed with 26 µL of 7.8 µM CLPFFD and 461.5 µL of sodium citrate 1.2 mM. The ratio CLPFFD to Aβ (1:24.5) is not enough to inhibit the fibril growth.

Irradiation

We used an HP HP83651B signal generator, working in a frequency range from 10 MHz to 50 GHz with a signal modulator HP8510C for determining the working frequency and power. Power was 100 mW. We apply the microwaves in a resonating chamber under mild magnetic stirring. The resonating chamber was a copper cavity of 6 cm diameter by 12 cm height with 0.5 cm thick walls. Microwaves arrived from the top through a waveguide while another waveguide read the signal inside the chamber. A resonant peak was chosen. Samples were introduced, and inside each vial a magnetic stirrer was introduced and the samples stirred for homogeneity. Samples and controls were irradiated for 10 and 30 min and then were centrifuged at 16,000*g* for 1 min and finally observed by TEM. Irradiated samples were incubated at room temperature for 48 h, and the fibril formation was determined by ThT test and by TEM.

Incubation of Irradiated Samples and Controls for Fibril Formation

The irradiated samples and controls and non-irradiated samples and controls were incubated at room temperature for 48 h to form amyloid fibrils.

Determination of Fibril Formation

Thioflavine T-test

Glycine 0.1 M buffer pH = 8.4 was introduced in 384 Nunc well fluorescence microliter plates and samples were added and mixed. Then Thioflavin T (100 µM) was added and mixed. The final peptide and Thioflavine T concentration is 4 µM. The fluorescence signal was measured (excitation wavelength 440 ± 10 nm) in a FL600 Microplate Fluorescence reader with KC4 version 2.7 software Biotek instruments, INC.

Transmission Electronic Microscopy

Aliquots of 10 µL (10 µM de Aβ) of the preparations were adsorbed for 1 min onto glow-discharged carbon-coated collodium films on 200-mesh copper grids. The TEM grids were then blotted and washed twice in distilled H_2O before

staining with uranyl acetate 2% for 2 min for visualization by TEM (JEOL JEM-1010).

Results and Discussion

We prepared Aβ PIAA with high amyloidogenic capacity according with Bieschke et al. [18]. The Aβ PIAA was incubated with AuNP-CLPFFD, forming the complex Aβ PIAA/AuNP-CLPFFD. The samples were then irradiated in a copper resonating chamber using a 14-GHz RF signal and 100 mW power. Aβ PIAA (10 μM) was mixed with AuNP-CLPFFD in two different ratios and the resulting complexes were characterized by TEM observing the typical PIAA structures, i.e., amylospheroids, protofibrils, and short fibrils attached and non-attached to AuNP-CLPFFD depending of the Aβ PIAA/AuNP-CLPFFD ratios (supplementary data, FS1). These complexes were irradiated for different times. After irradiation of Aβ PIAA/AuNP-CLPFFD samples, amorphous aggregate structures instead of the typical Aβ PIAA (amylospheroids, protofibrils, and short fibrils) were visualized by TEM (supplementary data, FS2). To determine whether Aβ PIAA lost the amyloidogenic potential, the irradiated samples were incubated for 48 h at room temperature to allow fibril formation and assess whether the amyloidogenic capacity of PIAA is altered. Thioflavine T (ThT) assays were performed to quantify the amount of fibrils in suspension, observing a fluorescence signal proportional to the amount of formed fibrils [19]. Figure 1 exhibits the fluorescence signal of irradiated samples and respective controls. A lower fluorescence signal was observed in Aβ PIAA/AuNP-CLPFFD complex samples compared with controls (Fig. 1). In addition, the irradiated sample (Aβ PIAA/AuNP-CLPFFD) incubation at room temperature was followed for 1 month but the intensity of fluorescence did not increase, which demonstrated that the fibrillogenic process had stopped (data not shown).

In samples irradiated for 10 min, a low fluorescence intensity signal was observed after 48 h of incubation (Fig. 1); some fibrils were visualized by TEM, which indicate that the irradiation time (10 min) was not enough to halt the amyloidogenic process (supplementary data, FS3). The halting of the fibrillogenic process is a concentration- and irradiation time-dependent phenomenon (supplementary data, FS3). Fibril formation was detected in irradiated samples with a high Aβ:AuNP-CLPFFD ratio (10 μM:0.2 nM) for 10 and 30 min (Fig. 2 and supporting material, FS3) but fibril formation was not detected using a final Aβ:AuNP-CLPFFD ratio of 10 μM: 1 nM and 30 min of irradiation (Figs. 1 and 3).

Figure 3 shows TEM micrographs of the sample Aβ PIAA/AuNP-CLPFFD complex and controls before and after irradiation for 30 min and further incubation (right), and non-irradiated and incubated sample and controls (left). The complex Aβ PIAA/AuNP-CLPFFD (Fig. 3b) was irradiated (Fig. 3c) and after incubation no fibril formation was observed (Fig. 3d). In contrast, in control experiments with irradiation, the fibril formation process was not interrupted (Fig. 3h, l, and p). We also carried out

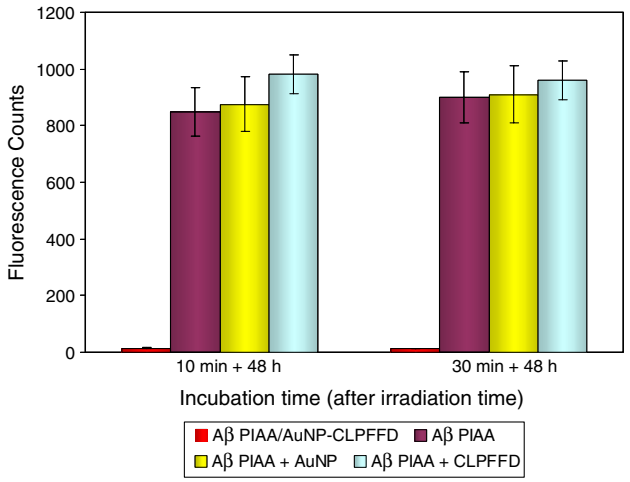

Fig. 1 Intensity of ThT fluorescence signal of Aβ PIAA/AuNP-CLPFFD sample (10 μM Aβ PIAA:1 nM AuNP-CLPFFD) and controls (Aβ PIAA, Aβ PIAA + CLPFFD, Aβ PIAA + bare AuNP) irradiated for 10 and 30 min and then incubated for 48 h

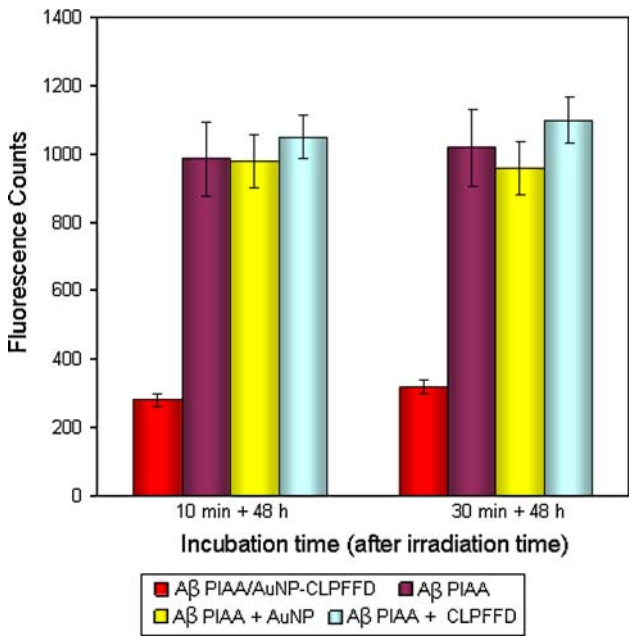

Fig. 2 Intensity of thioflavine T fluorescence signal of Aβ PIAA/AuNP-CLPFFD sample (10 μM Aβ PIAA:0.2 nM AuNP-CLPFFD) and controls Aβ PIAA (10 μM), Aβ PIAA + CLPFFD, Aβ PIAA + bare AuNP (Aβ 10 μM: 0.2 nM AuNP), irradiated for 10 and 30 min and then incubated for 48 h

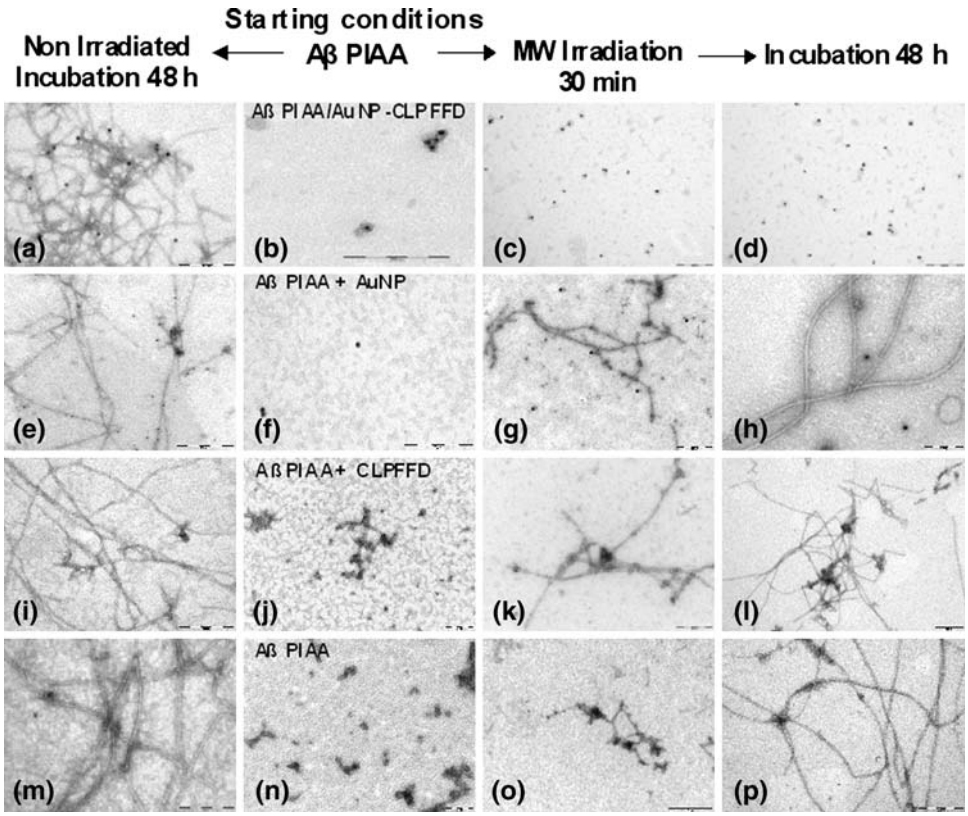

Fig. 3 TEM micrographs of Aβ PIAA/AuNP-CLPFFD sample and controls (starting conditions: **b**, **f**, **j**, and **n**, respectively). Sample and controls after irradiation for 30 min (**c**, **g**, **k**, and **o**, respectively) and incubated for 48 h at room temperature (**d**, **h**, **l**, and **p**, respectively). Non-irradiated sample and controls incubated for 48 h (**a**, **e**, **i**, and **m**, respectively). Bars represent 200 nm

control experiments to determine whether the presence of AuNP-CLPFFD, bare AuNP, or CLPFFD alone interfered with the normal fibrillogenic process of Aβ PIAA in the absence of irradiation (Fig. 3, left). In these cases, fibril formation was not inhibited (Figs. 3a, e, i, m, and 4). After irradiation of Aβ PIAA/AuNP-CLPFFD samples, non-characteristic structures corresponding to typical Aβ PIAA were visualized by TEM (Fig. 3c and additional figures in supplementary data, FS2). Irradiation in the presence of AuNP-CLPFFD produced dramatic effects on Aβ PIAA and consequently on the amyloidogenesis.

We studied the restoring of the amyloidogenic potential of irradiated Aβ PIAA/AuNP-CLPFFD after a denaturing treatment with 1,1,1,3,3,3-hexafluoro-2-propanol (HFIP) and incubation in water. Figure 5 shows a TEM micrograph of an irradiated Aβ PIAA/AuNP-CLPFFD sample before (Fig. 5a) and after (Fig. 5b) HFIP and incubation treatment and a non-irradiated control before (Fig. 5c) and after (Fig. 5d) HFIP and incubation treatment. Irradiation of Aβ PIAA/AuNP-CLPFFD provokes an irreversible effect that avoids restoration of Aβ fibrils formation in contrast to non-irradiated controls as summarized in Scheme 1.

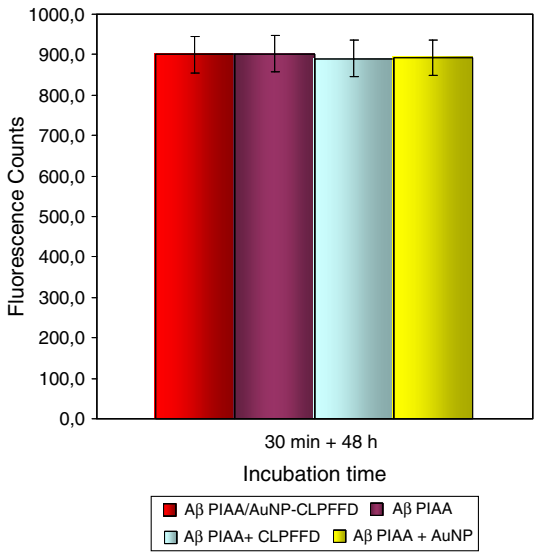

Fig. 4 Intensity of thioflavine T fluorescence signal of non-irradiated Aβ PIAA/AuNP-CLPFFD sample (10 μM Aβ PIAA:1 nM AuNP-CLPFFD) and controls Aβ PIAA (10 μM), Aβ PIAA + CLPFFD, Aβ PIAA + bare AuNP (Aβ 10 μM: 0.2 nM AuNP), stirred magnetically for 30 min and incubated for 48 h

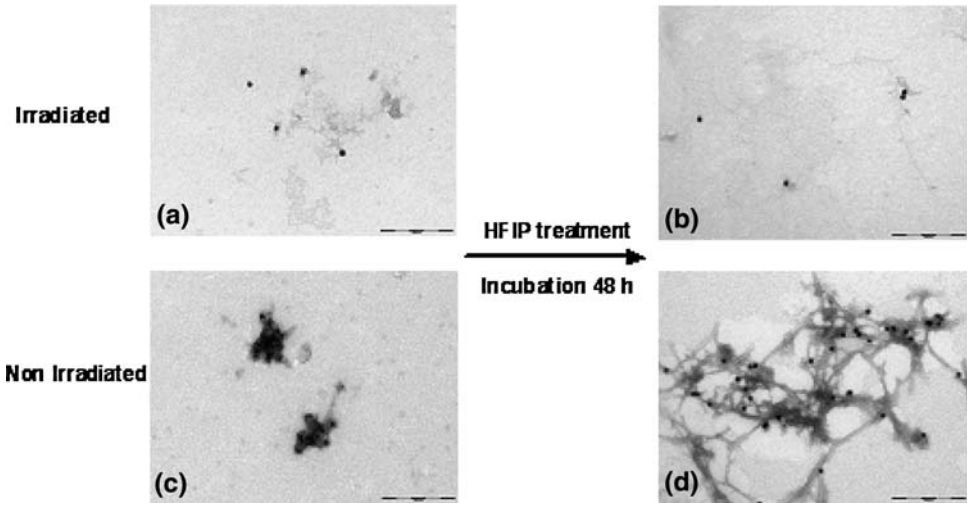

Fig. 5 TEM micrographs of irradiated sample of Aβ PIAA/AuNP-CLPFFD before (**a**) and after (**b**) treatment with HFIP and incubation for 48 h. Non-irradiated control (Aβ PIAA/AuNP-CLPFFD) before (**c**) and after (**d**) treatment with HFIP and incubation for 48 h. Bars represent 200 nm

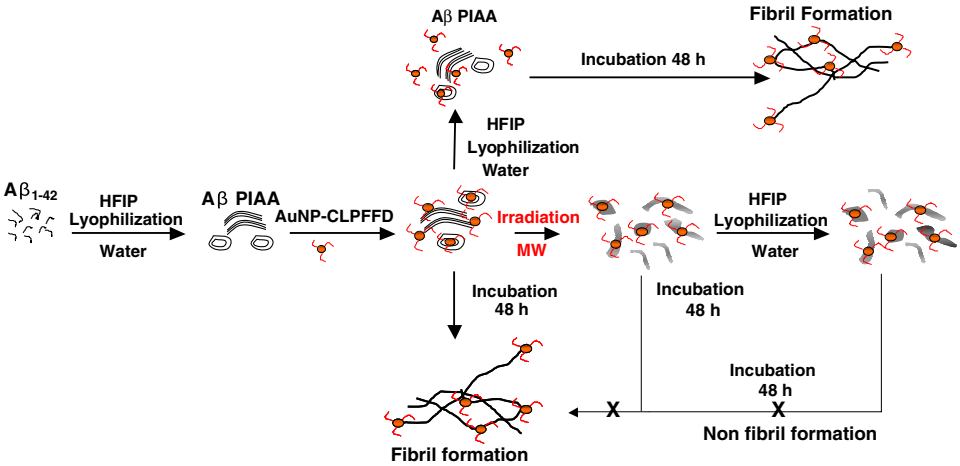

Scheme 1 Irreversible inhibition of the amyloidogenic process of Aβ PIAA mediated by AuNP-CLPFFD and MW

Could, However, the Irradiated Aβ PIAA/AuNP-CLPFFD Complex be Incorporated During Fibril Growth of Fresh Aβ PIAA?

We added fresh Aβ PIAA to both Aβ PIAA/AuNP-CLPFFD irradiated complex (sample) and Aβ PIAA/AuNP-CLPFFD non-irradiated complex (control), and incubated the resulting mixture for additional 48 h, determining fibril formation by ThT assay and by TEM. Figure 6a shows the time course of the fluorescence signal of sample and control. Although both have the same total Aβ concentration, fibril formation is lower in the former. The intensity of the fluorescence signal of the sample could be attributed only to fibril formation of the freshly added Aβ PIAA, while in control, the final fluorescence intensity corresponds to the addition of freshly added Aβ PIAA and Aβ PIAA/AuNP-CLPFFD together. Therefore, the species formed after irradiation are not amyloidogenic *per se* and they do not promote the formation of amyloid fibrils from freshly added Aβ PIAA solution either. Figure 6b–d shows fibril formation after freshly added Aβ PIAA aggregation in the presence of irradiated Aβ PIAA/AuNP-CLPFFD. Figure 6 shows that irradiated Aβ PIAA/AuNP-CLPFFD (Fig. 6b) are not bounded to fibrils (Fig. 6d), suggesting that irradiation of aggregates doped with AuNP-CLPFFD changes their structure in such a way that the new structure cannot be bound to the growing fibrils. In contrast, in non-irradiated control, Aβ PIAA/AuNP-CLPFFD is incorporated to the fibrils (Fig. 6 f, g), showing that AuNP-CLPFFD incorporation does not affect their growth. In conclusion, we can infer that the structure of Aβ PIAA/AuNP-CLPFFD is dramatically altered after irradiation and cannot be incorporated or bound to new Aβ fibrils.

Summing up, MW and AuNP linked to a peptide that selectively attaches to amyloidogenic A$\beta_{1–42}$ structures inhibit irreversibly their normal aggregation. The resulting irradiated products are not amyloidogenic. Our approach provides a viable means to inhibit irreversibly the

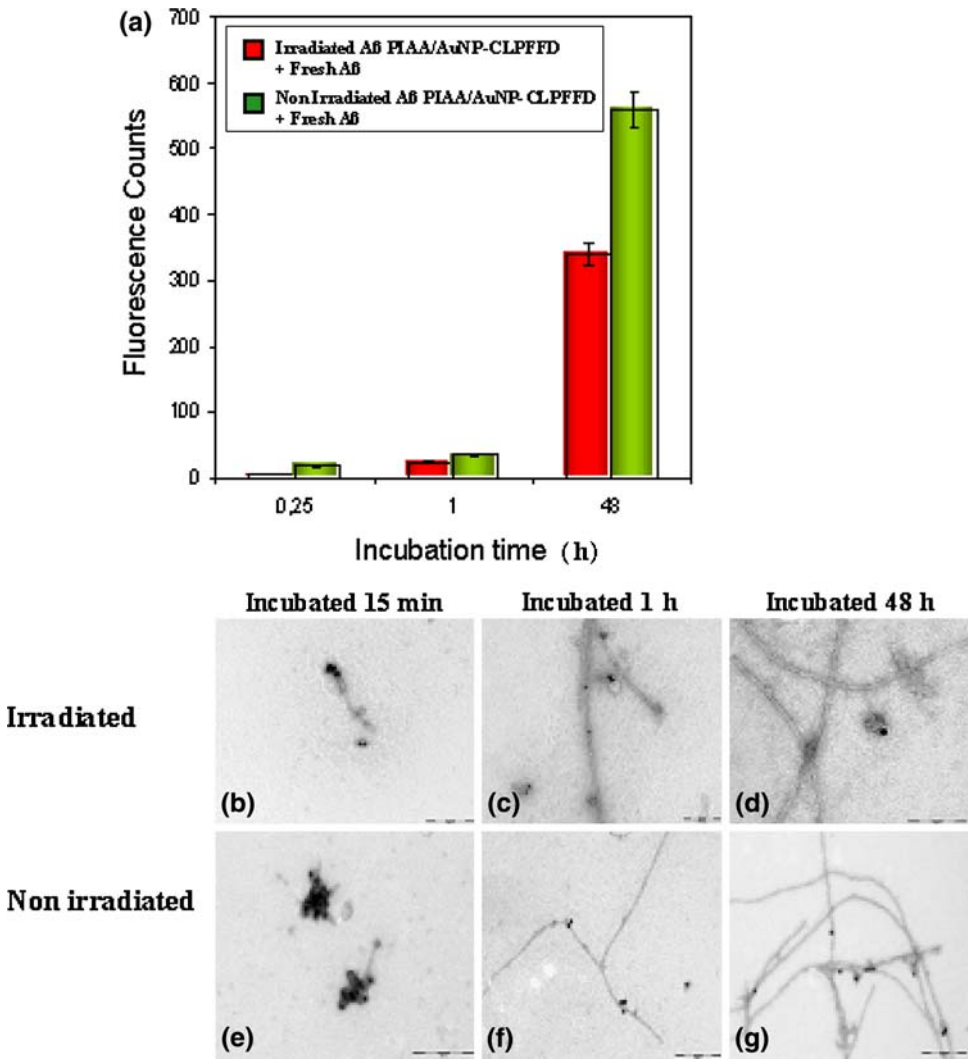

Fig. 6 Time course of fluorescence ThT signal of freshly added Aβ PIAA in the presence of Aβ PIAA/AuNP-CLPFFD sample (irradiated) and control (non-irradiated) (**a**). TEM micrograph of freshly added Aβ PIAA (3.7 μM) incubated with irradiated Aβ PIAA (2.2 μM)/AuNP-CLPFFD for 15 min (**b**), 1 h (**c**), and 48 h (**d**). TEM micrograph of freshly added Aβ PIAA (3.7 μM) incubated with non irradiated Aβ PIAA(2.2 μM)/AuNP-CLPFFD for 15 min (**e**), 1 h (**f**), and 48 h (**g**). Bars represent 200 nm

amyloidogenic process of Aβ. Further investigations in our laboratory include an assessment of the irradiation effect on Aβ structure and potential toxicity. This tool could be used for therapeutical purposes by inhibiting locally and remotely the amyloidogenic process of proteins.

Acknowledgments We acknowledge Elisenda Coll of Servei Cientific-Tecnics (Universitat de Barcelona) for assistance in TEM observations and Aurora Morales for XPS asignations. This work was supported by FONDECYT 1061142, FONDAP 11980002 (17 07 0002), and AECI A/010967/07.

References

1. R.M. Murphy, Biochim. Biophys. Acta Biomembranes **1768**, 1923 (2007)
2. M. Arimon, I. Diez-Perez, M.J. Kogan, N. Durany, E. Giralt, F. Sanz et al., FASEB J. **19**, 1344 (2005)
3. M.J. Kogan, N.G. Bastus, R. Amigo, D. Grillo-Bosch, E. Araya, A. Turiel, A. Labarta, E. Giralt, V.F. Puntes, Nano Lett. **6**, 110 (2006). doi:10.1021/nl0516862
4. N.G. Bastús, M.J. Kogan, R. Amigó, D. Grilló-Bosch, E. Araya, A. Turiel et al., Mater. Sci. Eng. C **27**, 1236 (2007). doi:10.1016/j.msec.2006.08.003
5. I. Olmedo, E. Araya, F. Sanz, E. Medina, J. Arbiol, P. Toledo, A. Álvarez-Lueje, E. Giralt, M.J. Kogan, Bioconjugate Chem. **19**(6), 1154 (2008)
6. R. Kayed, E. Head, J.L. Thompson, T.M. McIntire, S.C. Milton, C.G. Glabe, Science **300**, 486 (2003)
7. D. Walsh, D.J. Selkoe, J. Neurochem. **101**, 1172 (2007). doi:10.1111/j.1471-4159.2006.04426.x
8. E. Masliah, Nature **451**, 638 (2008)
9. L.D. Estrada, C. Soto, Curr. Top. Med. Chem. **7**, 115 (2007). doi:10.2174/156802607779318262
10. A. Rauk, Dalton Trans. 1273 (2007)
11. M.A. Rojavin, M.C. Ziskin, Q. J. Med. **91**, 57 (1998)
12. S. Banik, S. Bandyopadhyay, S. Ganguly, Bioresour. Technol. **87**, 155 (2003). doi:10.1016/S0960-8524(02)00169-4
13. A.G. Pakhomov, Y. Akyel, O.N. Pakhomova, B.E. Stuck, M.R. Murphy, Bioelectromagnetics **19**, 393 (2001)

14. E.G. Novoselova, E.E. Fesenko, V.R. Makar, V.B. Sadovniko, Bioelectrochem. Bioenerg. **49**, 37 (1999). doi:10.1016/S0302-4598(99)00059-8
15. H. Bohr, J. Bohr, Phys. Rev. **61**, 4310 (2000)
16. C. Alexiou, W. Arnold, R.J. Klein, F.G. Parak, P. Hulin, C. Bergemann et al., Cancer Res. **60**, 6641 (2000)
17. B. Permanne, C. Adessi, G.P. Saborio, S. Fraga, M.J. Frossard, J. Van Dorpe et al., FASEB J. **16**, 860 (2002)
18. J. Bieschke, S.J. Siegel, Y. Fu, J.W. Kelly, Biochemistry **47**, 50 (2008). doi:10.1021/bi701757v
19. H. LeVine, Protein Sci. **2**, 404 (1993)